Recent progress of GEANT4 electromagnetic physics for LHC and other applications

A Bagulya[1], J M C Brown[2], H Burkhardt[3], V Grichine[1], S Guatelli[4], S Incerti[5,6], V N Ivanchenko[3,7], O Kadri[8], M Karamitros[6], M Maire[7,9], K Mashtakov[10], M Novak[3], L Pandola[11], P G Rancoita[12], D Sawkey[13], M Tacconi[12,14], L Urban[7]

[1]Lebedev Physical Institute, Leninskii Pr. 53, Moscow 119991, Russia
[2]Queen's University Belfast, School of Mathematics and Physics, University Road, Belfast, Northern Ireland BT 7 1NN, United Kingdom
[3]CERN, 1211 Genéve 23, Switzerland
[4]University of Wollongong, Centre for Medical Radiation Physics, Northfields Avenue, Wollongong, NSW 2522, Australia
[5]CNRS-IN2P3, CENBG, UMR 5797, F-33170 Gradignan, France
[6]Université Bordeaux, CENBG, UMR 5797, F-33170 Gradignan, France
[7]Geant4 Associates International Ltd., United Kingdom
[8]King Saud University, Riyadh, Saudi Arabia
[9]IN2P3/LAPP, 74941 Annecy-le-vieux, France
[10]University of the West Scotland, Paisly Campus, Paisley, United Kingdom
[11]INFN, Laboratori Nazionali del Sud, I-95123 Catania, Italy
[12]INFN, Milano-Bicocca, Milano, Italy
[13]Varian Medical Systems, 3120 Hansen Way, Palo Alto, CA 94304, USA
[14]University Milano-Bicocca, Milano, Italy

E-mail: `Vladimir.Ivantchenko@cern.ch`

Abstract. We report on recent progress of the GEANT4 electromagnetic physics sub-packages. Several new interfaces and models recently introduced are already used in LHC applications and may be useful for any type of simulation. Significant developments were carried out to improve the user interface, develop models of single and multiple scattering, and validate high energy models. Part of these developments are included in the GEANT4 10.2 release and the full set are available in the new version 10.3 of December, 2016.

1. Introduction

GEANT4 electromagnetic (EM) physics libraries were described in detail in reviews [1], [2]. The recent developments for standard EM sub-libraries were driven by two main requirements: to improve the accuracy and robustness for ongoing Large Hadron Collider (LHC) experiments, and to enable the possibility of simulating various variants of Future Circular Collider (FCC) interaction regions and detectors. In the low-energy region, modifications were mostly done for multiple and single scattering, atomic de-excitation, and for development of low energy models for GEANT4 DNA [3]. In this work we will discuss selected developments and show some validation results mainly relevant to LHC and FCC obtained for GEANT4 10.2 and 10.3.

2. EM sub-package infrastructure upgrades

A new concept of EM parameter definition has been implemented. This was needed because the old approach shows some difficulties in the multithreaded mode. All EM parameters can now be defined in C++ code or user interface (UI) in the GEANT4 PreInit and Idle states. In addition, several new parameters have been added.

The user may now define the lowest energies for tracking of e^+/e^- and muons/hadrons. At the end of a step kinetic energy of a charged particle is checked and if it is below the limit, the particle's post-step kinetic energy is set to zero and the energy is added to the local energy deposition. This approach permitted the removal from some models of similar limitations which were not transparent to users.

Specific models [2], including photo-absorption ionization (PAI), microelectronics (Micro-Elec), and DNA, may be used per geometry region, and the physics configuration of a GEANT4 reference physics list may be used for a specific region (e.g. where higher precision is required, such as a tracker or a specific calorimeter). These new UI commands are:

- */process/em/AddPAIRegion particle myregion PAI*
- */process/em/AddDNARegion myregion DNAtype*
- */process/em/AddMicroElecRegion myregion*
- */process/em/AddEmRegion myregion EMtype*
- */process/em/printParameters*

Here *myregion* is the name of *G4Region*; *DNAtype* is the name of the DNA physics constructor; *EMtype* is the name of an existing EM physics constructor (for example, *G4EmStandard_opt4*). It is recommended to first instantiate the physics list, then redefine specific custom parameters. Also, the C++ interface and UI commands are only active for the master thread. The *G4EmProcessOptions* class still exists in the GEANT4 distribution, but it is considered deprecated and the recommendation is to not use it anymore, especially for applications running in the multithreaded mode.

The upper limit of EM models was extended from 10 TeV to 100 TeV to allow for FCC design studies. The increase of this limit means that the EM tables built in the initialisation phase of GEANT4 require about 10% more memory, and a similar increase in CPU time is required for initialisation. However, in a concrete user application this upper limit may be reduced accourding to the use case in order to reduce CPU of initialisation and allocated memory.

Rare EM processes [4], [5] (important for FCC design) may be now enabled on top of any reference physics list via new UI commands. Also existing physics list commands were reviewed and the new set for GEANT4 10.3 is:

- */physics_list/em/SyncRadiation true/false*
- */physics_list/em/SyncRadiationAll true/false*
- */physics_list/em/GammaToMuons true/false*
- */physics_list/em/PositronToMuons true/false*
- */physics_list/em/PositronToHadrons true/false*

3. Model developments

More accurate simulation of EM shower profiles for LHC experiments requires review and improvements on the per mille level. This is important for high statistics run-2 analysis and other applications.

3.1. Bremsstrahlung: improved implementation of the LPM effect

Gamma emission for electron and positron bremsstrahlung [6] has been reviewed, with a focus on the Landau-Pomeranchuk-Migdal (LPM) effect. The LPM model is now fully consistent with the Migdal model, and there is an improved agreement between simulation and data. Figure 1 shows the emission for 25 GeV e^- incident on lead [7], and 207 GeV e^- incident on iridium [8]. Results with GEANT4 version 10.3.beta are in good agreement with measurement. This improvement slightly narrows EM shower but the change is difficult to observe when macro parameters are studied: for example, R_9 distribution (ratio of energy deposition in a crystal matrix $R_9 = E_{3x3}/E_{5x5}$) for CMS-type crystal calorimeter is practically unchanged.

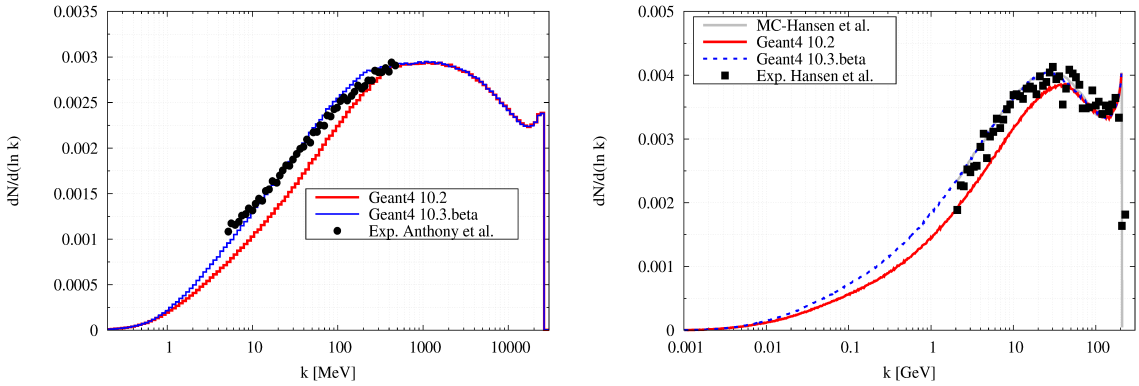

Figure 1. Number of photons produced per energy bin for 25 GeV e^- incident on a 0.15 mm thick Pb target (left), and 207 GeV e^- incident on a 0.128 mm thick Ir target (right). Points - data [7], [8], lines - Geant4 simulation.

3.2. Multiple and single scattering

Models of single and multiple scattering were under developments during the recent years [9]. As a result, a following combiidnation of models is used as a default since GEANT4 10.0 [10]:

- for e^+, e^- below 100 MeV Urban model of multiple scattering;
- for e^+, e^- above 100 MeV, for protons, anti-protons, muons, pions, and kaons a combination of *G4WentzelVIModel* of multiple scattering for small angles and *G4eSingleScatteringModel* single scattering model for large angles (WVI-SS);
- for other particles Urban model.

The limit angle between multiple and single scattering (SS) is computed dynamically. It depends on the momentum of a particle and step size. This configuration is working well for several multiple scattering benchmarks but accurate simulation for low-energy electrons requires too many steps in the vicinity of the geometry boundary. In order to improve precision and CPU performance of electron transport the developments of the *G4GoudsmitSandersonMscModel* (GS) was initiated [11].

Now we report, that the implementation of GS has been reviewed and rewritten for GEANT4 10.2. The model is a combination of the Goudsmit-Saunderson multiple scattering theory [12] with Rutherford differential cross sections, implemented according to the Kawrakow-Bielejaw [13], [14] hybrid model. Probability density functions (PDFs) are pre-computed on a two-dimensional grid, and a variable transformation is used to create smooth PDFs. This leads to accurate and robust sampling. The range factor used to limit the step length can be

set to any value, with 0.2 as the default, because the true step length is limited to the first transport mean free path. Boundaries are only reached in single scattering mode. The physics accuracy of GS is on the same level as the default Urban model. This can be seen in various validation tests, in particular, electron scattering in thin foils, energy deposit versus depth for low energy electrons, and the high energy calorimeter response. Computation times are similar to, or better than, those with the Urban model. The main advantage of GS is that it does not have tuned parameters.

Figure 2 shows that the accuracy of the updated GS model for heavy media is comparable to WVI-SS and the single scattering model (SS). The GS curve is close to the data compare to Opt3 configuration, which is implemented in *G4EmStandardPhysics_option3* EM physics constructor using Urban model for all particles and a strict limitation on the step size. The current default Opt0 configuration provide less accurate results but for Opt0 much less CPU is required for this setup, GS and Opt3 in this case are approximately two times slower. The WVI-SS combination is not optimised for low energy electron transport, so it is providing good results but is even much slower for this setup. Recently, results of measurements for few GeV e^- beam scattering in thin

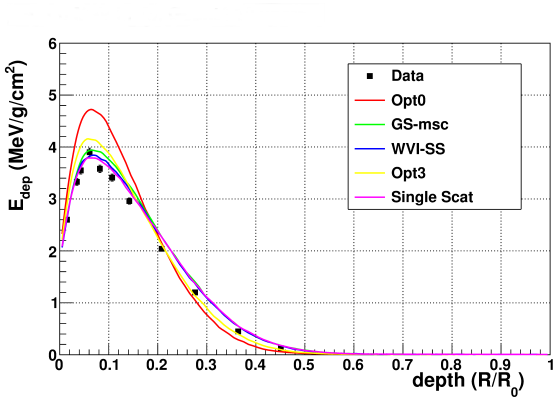

Figure 2. Dose deposit as a function of normalized depth for 1 MeV e^- incident on Ta for GEANT4 version 10.3, for different EM physics lists compared to measured data [15].

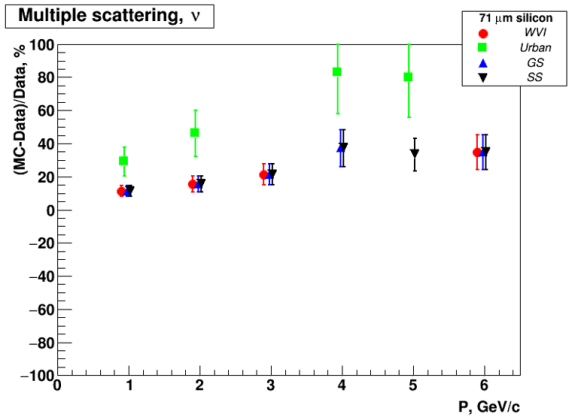

Figure 3. Simulation versus data [16] for the parameter ν of the fit function for scattering of e^- off 71 μ m Si as a function of beam momentum.

silicon layers were published [16]. In this work, instead of recommended physics list a custom one with only Urban model was considered. We repeated the same procedure as described in this manuscript and confirm that the tail parameter of such fit obtained with the Urban model does not well agree with the data (Figure 3). At the same time, GS, SS and WVI models are in much better agreement.

3.3. Nuclear form-factor parameterisation

The differential cross section of EM processes includes a nuclear form factor (FF) accounting for spatial distribution of charge density. Until now, all scattering models used an exponential charge distribution for the form factor. In GEANT4 version 10.3, the form factor may be either exponential, Gaussian, flat, or none. The form factor may be selected using the new UI command

- */process/em/setNuclearFormFactor FF_type*
- *FF_type = None/Exponential/Gaussian/Flat*

Now any GEANT4 model may use this form factor for cross section computation and/or sampling of final state. In particular, in the current GEANT4 default physics configurations of multiple and single scattering models WVI-SS this types are used.

The new single scattering class *G4eSingleCoulombScatteringModel* (ESS) implements the screened relativistic treatment [17], [18] of the Mott cross section for electrons incident on a nucleus. This treatment accounts for effects due to the screened Coulomb fields, finite sizes and rest masses of nuclei. Note, that the Mott corrections are not taken into account in the default GEANT4 models. The calculation of the scattering parameters is performed in the center of mass system and Lorentz transformations are applied to obtain the energy and momentum quantities in the laboratory system after scattering. The differential cross section [17], [19] is given by:

$$\frac{d\sigma(\theta)}{d\Omega} = \left(\frac{Ze^2}{\mu c^2 \beta^2 \gamma}\right)^2 \frac{R_{Mott}|F_N(q)|^2}{(2A_s + 2\sin^2(\theta/2))^2}. \quad (1)$$

where Z is the atomic number of the target nucleus, $\mu = m\frac{Mc^2}{E_{cm}}$ is the relativistic reduced mass of the system, m and M are rest masses of the electron and of the target nuclei respectively, and E_{cm} is the total center of mass energy; A_s is the screening coefficient [20]; R_{Mott} is the ratio of the Mott to Rutherford differential cross section obtained by an analytical fit [21]; $F_N(q)$ is the nuclear form factor. The importance of the form factor, especially at high scattering angles, is shown in figure 4. This model, with the factorization of the screening term, is suitable for

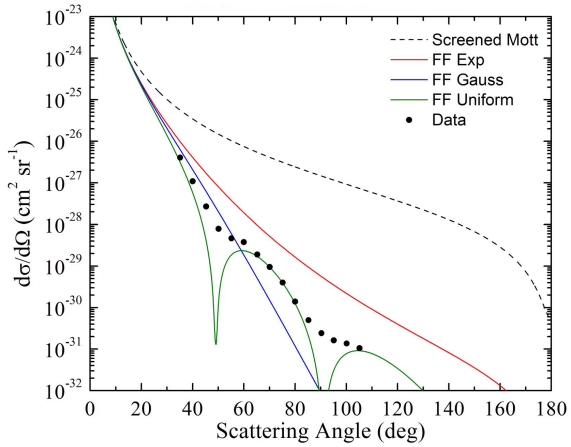

Figure 4. Differential cross section as a function of the scattering angle for 183 MeV electrons in indium. Points are data [22], lines are simulation with different form factor options: none - black, exponential - red, Gaussian - blue, flat - green.

incident electrons with energy above 200 keV. Screening and spin effects are separately treated in Equation 1. Zeitler and Olsen [23] suggested that for electron energies above 200 keV the overlap of spin and screening effects is small for all elements and for all energies; for lower energies the overlapping of the spin and screening effects may be appreciable for heavy elements and large angles.

ESS allows obtaining both the nuclear stopping power, non-ionizing energy loss (NIEL), the new direction of the incoming particle, and the energy transferred to the target atom of the material. If the transferred energy is greater than the threshold energy needed to displace an atom, a secondary recoil ion is generated. In the user analysis, the kinetic energy of the secondary particles may be multiplied by the Norgett-Robinson-Torrens expression [24], [25] that approximates the Lindhard partition function to obtain the NIEL deposited in the target material, moreover nuclear stopping power may be computed.

3.4. Relativistic corrections for muon scattering

For scattering of high energy charged particles, nuclear recoil may be important. Figure 5 shows results of simulation using default SS model and an alternative *G4hSingleScatteringModel* for simulation of muon scattering in a thin silicon layer. The new model uses the same approach [17] for description of two-body scattering problem as the single scattering model described in the previous sub-chapter. The effect of relativistic corrections may be better identified in the ratio of two distributions, where it is seen that corrections affect mainly central part of the angular distribution. This study confirms that for high energy simulation it is enough to add relativistic corrections to the default models instead of creation of a special models for high energy.

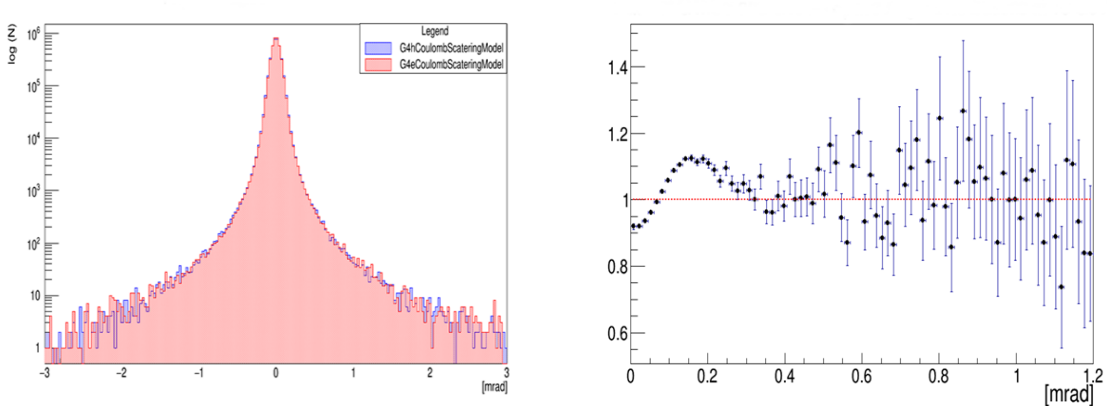

Figure 5. Simulation of 10 GeV muon scattering of 300 μm silicon for two single scattering models (left) and the ratio of two distributions (right).

3.5. Low energy models

Initialisation of the atomic de-excitation module was revised and several new options were added. In particular, the possibilities of simulating full Auger cascades, full gamma casacde and using astrophysical data for fluorescence are available. New UI commands can be used on top of any reference physics list

- */process/em/augerCascade true/false*
- */process/em/fluoBearden true/false*
- */process/em/deexcitationIgnoreCut true/false*

An extensive developments were carried out for simulation of effects of radiation at cellular level (Geant4 DNA). New models are added and software infrastructure is extended. As a product of common development for EM interfaces and DNA models development, a study of electron transport where standard and DNA models work in one setup become possible [26].

4. New validation results

Validation of EM physics is a contunues Geant4 task which is been carried out permanently [27]. In this work we report only few selected results but the full set of EM benchmarking is available in Geant4 web pages.

Electron multiple scattering is validated at 13 and 20 MeV by comparison of simulations to a thin foil scattering benchmark [28]. One comparison is the width of the central Gaussian peak. Figure 6 shows the ratio of simulated to measured peak widths at 13 MeV for each scattering target, using Geant4 version 10.2.patch2. Results with the Urban model are typically within

2% of the measured values. The GS model shows larger discrepancies of up to 6% for the C target. In general, the central peak widths in the GS simulations are narrower than measured. Figure 7 shows the ratio of simulated fluence to measured fluence, for three scattering models. (Because the normalization of the measured data is not known, the measured data were scaled for each simulation to minimize the disagreement between measurement and simulation.) In general, GS agrees well with SS model. Both GS and SS show more fluence in the central region than the measurement, and less fluence in the tails. In contrast, the Urban model shows less fluence in the central region, and more in the tails. Overall, the Urban results are in better agreement with the measured data than the GS results are, and the GS results are in better agreement with SS. This likely results from the Urban model being tuned to give a good match to these measurements. The electromagnetic shower simulation is stable beween recent

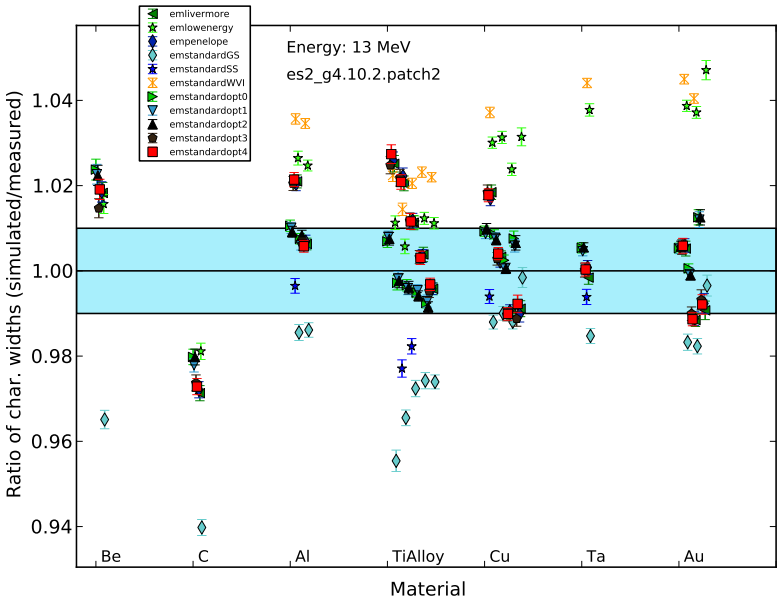

Figure 6. The ratio of the simulated to measured width [28] of the central peak of the scattered e^- beam for the 13 MeV simulation, for different scattering targets and physics lists.

GEANT4 versions. In particular, energy resolution is stable (Figure 8). In this plot, measured resolutions of two lead/scintillator sampling calorimeters as a function of range cut are shown for the default EM physics and for the case, when GS is used for simulation of e^+, e^- multiple scattering below 100 MeV. The results with GS model are competitive for the high sampling fraction calorimeter. For the low sampling fraction calorimeter, the resolution obtained with GS is lower than measurements. Studies of factors affecting simulation resolution are ongoing.

5. Conclusions

GEANT4 EM sub-libraries were updated for 10.2 and 10.3 versions. Main improvements were introduced for multiple and single scattering models. Results for main applications are stable. The upper energy limit is extended from 10 to 100 TeV. New user interfaces allowing to define physics per geometry region via UI commands.

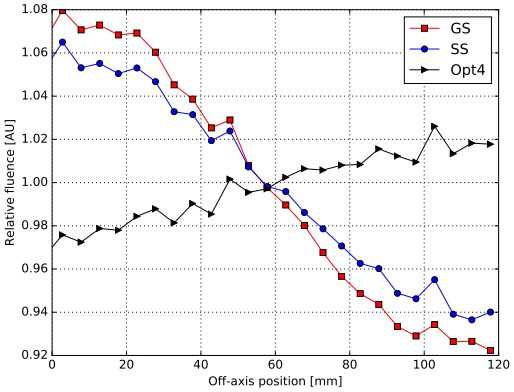

Figure 7. Ratio of the simulated fluence to measured fluence for the 82.4 μm thick Ti alloy target as a function of distance from the central axis.

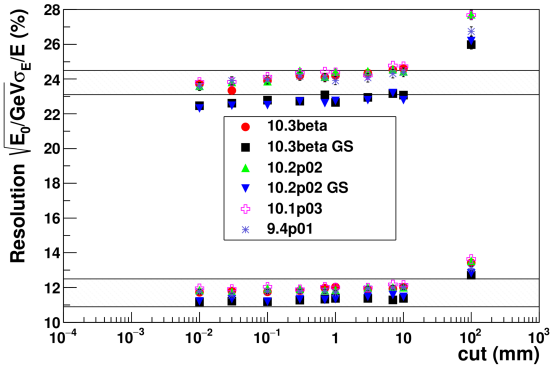

Figure 8. e^- 10 GeV in Pb/Scin sampling calorimeters: points are simulation with different GEANT4 versions; bands are one standard deviations uncertainty of data [29], [30].

References

*

[1] Agostinelli S et al. 2003 *Nucl. Instrum. Methods A* 506 250-303
[2] Allison J et al. 2016 *Nucl. Instrum. Methods Phys. Res. A* 835 186-225
[3] Bernal M A et al. 2015 *Phys. Med.* 31 861-74
[4] Bogdanov A G et al. 2006 *IEEE Trans. Nucl. Sci.* 53 513-9
[5] Apostolakis J et al. 2015 *J. Phys: Conf. Ser.* 664 072021
[6] Allison J et al. 2012 *J. Phys: Conf. Ser.* 396 022013
[7] Anthony P L et al. 1997 *Phys. Rev. D* 56 1373
[8] Hansen H D et al. 2004 *Phys. Rev. D* 69 032001
[9] Ivanchenko V N, Kadri O, Maire M and Urban L 2010 *J. Phys.: Conf. Ser.* 219 032045
[10] Ivanchenko V N et al. 2014 *J. Phys.: Conf. Ser.* 513 022015
[11] Kadri O, Ivanchenko V, Gharbi F and Trabelsi A 2009 *Nucl. Instrum. and Meth. B* 267 3624-32
[12] Goudsmit S and Saunderson J L 1940 *Phys. Rev.* 57, 24
[13] Bielajew A F 1996 *Nucl. Instrum. Methods Phys. Res. B* 111 195
[14] Kawrakow I and Bielajew A F 1998 *Nucl. Instrum. Methods Phys. Res. B* 134 325
[15] Lockwood G J et al. 1987 Calorimetric Measurement of Electron, Energy Deposition in Extended Media Theory vs. Experiment *SANDIA REPORT SAND79-0414.UC-34a*
[16] Berger N et al. 2014 *JINST* 9 P07007
[17] Boschini M J et al., 2011 Nuclear and Non-Ionizing Energy-Loss of electrons with low and relativistic energies in materials and space environment, *Proc. of the 13th ICATPP Conference* (World Scientific, Singapore) pp 961-82 *IBSN: 978-981-4405-06-5*
[18] Boschini M J, Rancoita P G and Tacconi M 2016 SR-NIEL Calculator: http://www.sr-niel.org/
[19] Leroy C and Rancoita P G, 2016 Principles of Radiation Interaction in Matter and Detection 4th Edition *World Scientific. Singapore ISBN-978-981-4603-18-8* (printed); *ISBN.978-981-4603-19-5* (ebook)
[20] Moliere G 1947 *Z. Naturforsh A* 2 133-45; 3 78.
[21] Boschini M J et al. 2013 *Rad. Phys. Chem.* 90 39-66; *doi: 10.1016/j.radphyschem.2013.04.020*
[22] Hahn B et al. 1956 *Phys. Rev.* 101 1131
[23] Zeitler E and Olsen A 1956 *Phys. Rev.* 136 A1546-52
[24] Jun I 2001 *IEEE Trans. on Nucl. Sci.* 48 16275
[25] Messenger S R et al. 2003 *IEEE Trans. on Nucl. Sci.* 50 1919-23
[26] Sakata D et al. 2016 *J. Appl. Phys.* 120 244901; doi: 10.1063/1.4972191
[27] Apostolakis J et al. 2010 *J. Phys: Conf. Ser.* 219 032044
[28] Ross C K, McEwen M R, McDonald A F, Cojocaru C D and Faddegon B A 2008 *Med. Phys.* 35 4121
[29] Bernardi E et al. 1987 *Nucl. Inst. Meth. A* 262 229-42
[30] D´ Agostini G et al., 1989 *Nucl. Inst. Meth. A* 274 134